A Study on Negative Poisson's Ratio Effect of 3D Auxetic Orthogonal Textile Composites under Compression

Jifang Zeng, Hong Hu*, Lin Zhou

Institute of Textiles and Clothing, The Hong Kong Polytechnic University, Hung Hom, Hong Kong

*Corresponding author: tchuhong@polyu.edu.hk

Abstract. More and more researches have been focused on auxetic composite materials and a number of composite structures have been fabricated, synthesized or theoretically predicted. Since their structures are complex, their mechanical behavior is very difficult to be characterized. The purpose of the present paper is to systematically investigate the negative Poisson's ratio effect of a novel three dimensional (3D) auxetic orthogonal textile composite under compression. Firstly, a set of equations are derived for the theoretical calculation of the Poisson's ratio of the composite under uniaxial compression via an analytical analysis. Secondly, a finite element model (FEM) is created by ANSYS Parameter Design Language (APDL) and is verified by experiment. The deviation between the simulation and experimental results are carefully discussed. Thirdly, the effects of geometry parameters and material properties on the negative Poisson's ratio behavior of the composite are discussed based on the FEM simulated results. At last, a general basis is concluded. It is expected that the outcomes of this study could be useful to guide the fabrication of auxetic textile composites with required negative Poisson's ratio behavior.

Key words: 3D auxetic textile composite, ANSYS, Finite element model, Negative Poisson's ratio effect

1. Introduction

Contrary to positive Poisson's ratio materials, negative Poisson's ratio materials (called also auxetic materials) are laterally expand when longitudinally stretched or laterally contract when longitudinally compressed. Due to this non-conventional behavior, auxetic materials exhibit an improved bear resistance, which makes them to be a good choice for fabricating protective structure. Besides, they are also facilitating

to form various complex shapes due to synclastic curvature under bending. However, auxetic materials are rare in nature. Many efforts have been made for the fabrication of auxetic materials and structures such as porous materials, composites and cellular solids.

Lakes first reported auxetic polyurethane (PU) foams with re-entrant structures in 1987[1], and later made a comprehensive review on auxetic materials including their fabrication methods, mechanical properties and research advances in 1993[2]. Since then, a plenty of auxetic materials have been fabricated, such as micro-porous polytetra-fluorethylene (PTFE)[3, 4], polypropylene (PP)[5], microporous ultra high molecular weight polyethylene (UHMWPE)[6] and auxetic open cell PU foams[7]. Usually, the negative Poisson's ratio composites were fabricated through appropriate structural design using positive Poisson's ratio materials, and more and more attentions are focused on their mechanism and properties. As reported by Alderson et al.[8], there are two main methods for producing auxetic composite materials: the use of re-entrance of auxetic reinforcements[9] and adoption of specially designed configurations using conventional components. By a simple analysis using two-dimensional (2D) lamination theory in combination with the appropriate three-dimensional (3D) anisotropic constitutive equation, Herakovich[10] found that the Poisson's ratio of a graphite-epoxy laminate ranged from 0.49 to -0.21. Milton[11] suggested a conclusive proof that the Poisson's ratio of isotropic materials could approach to -1 by layering the component materials together in different directions at widely separated length scales. Luzhuo Chen et al.[12]fabricated an auxetic composite

by embedding the carbon nanotube (CNT) into the polymer. The Poisson's ratio of this CNT/polymer composite could be down to -0.50 and predicted by a theoretical model under stretching. Paul Michelis and Vasilios Spitas[13] conducted a numerical and experimental analysis on the auxetic behavior of a directionally reinforced integrated single yarn (DIRIS) architecture with a reinforcement of glass or carbon fibers. Compared with classical isogrid honeycomb with similar fiber content, the DIRIS auxetic core and panel performed much better on flexural and shear test. Recently, Ge et al.[14-16] proposed a 3D auxetic textile structure formed with 3D orthogonal reinforcements. They numerically investigated the Poisson's ratio of this structure using a unit cell for undeformed and deformed warp yarn at the initial state, respectively. By eliminating the stitch yarn in the former 3D auxetic textile structure[15], Jiang et al.[17] fabricated a similar orthogonal auxetic composite using ABS tube and polyester filament as reinforcements and PU foam as matrix. They proposed an implicit equation to calculate the Poisson's ratio without considering the diameter of weft yarn. Lin Zhou et al.[18] experimentally studied the mechanical behavior of 3D orthogonal textile composites. They found that the mechanical behavior strongly relied on the arrangement of yarns and the value of negative Poisson's ratio of the 3D auxetic composite could be adjusted by the geometry of reinforcements.

Inspired by this, the aim of this work is to systematically investigate the negative Poisson's ratio effect of 3D auxetic textile composites made with different geometry parameters and material properties of reinforcements under uniaxial compression via

both the theoretical and numerical approaches. Based on the theoretical analysis for a unit cell fabricated with undeformed warp yarn and inextensible weft yarn, a simplified equation is firstly derived for calculating the Poisson's ratio as a function of compression strain. Then, the calculated Poisson's ratio is compared with 2D FEM simulation results. The difference between them is analyzed and the source of bias is also evaluated. Before the investigation of geometry and material effects, the accuracy of 2D FEM simulation is verified by experimental results. After the validation, the 2D FEM model is finally used to predict the effects of warp yarn spacing, diameters of warp and weft yarn, and mechanical properties of warp and weft yarn on negative Poisson's ratio behavior of the composite. It is expected that the outcomes of this study could be useful to guide the fabrication of auxetic textile composites.

2. Materials and methods

2.1 Material properties and structure

In this study, a 3D orthogonal textile structure formed with warp, weft and stitch yarns are used as reinforcements, and PU foam is used as the matrix to fabricate auxetic composite, as shown in Fig.1a. For brevity, the fabrication of the composite structure is not included in this article. The details of the fabrication process have been illustrated by Zhou et al. [18]. The skeleton of this textile structure is made by orthogonally layered warp and weft yarns. As shown in Fig.1b, the warp and yarns are stacked in parallel layer by layer in the *XOZ* plane and bound up together by stitch yarns in *Y* direction. While a warp yarn is arranged in the center of two warp yarns

located in its adjacent layer, the weft yarns are arranged uniformly layer by layer and the number of weft yarns is kept the same in every layer. Thus, the geometry of this auxetic textile reinforcement structure is determined by the diameter of warp yarns D_1, the total number of warp yarn N_0, the diameter of weft yarns D_2, the total number of weft yarn N_1, the warp yarn spacing S_x, the weft yarn spacing S_z and the dimension of composites in X, Y and Z direction. Obviously, the deformation behavior of auxetic textile composite can be characterized from the plane shown in Fig.1c.

(a)

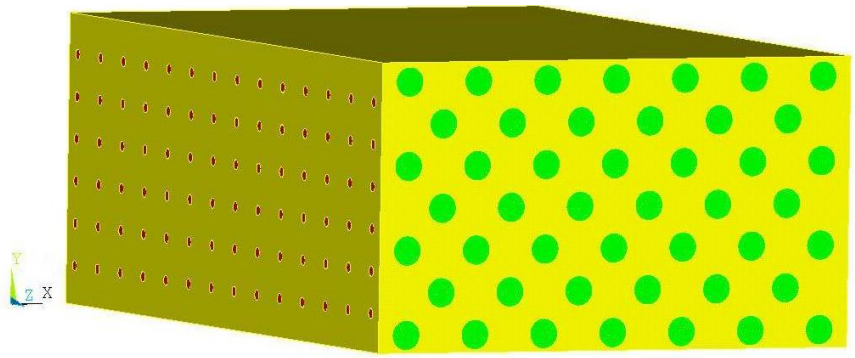

(b)

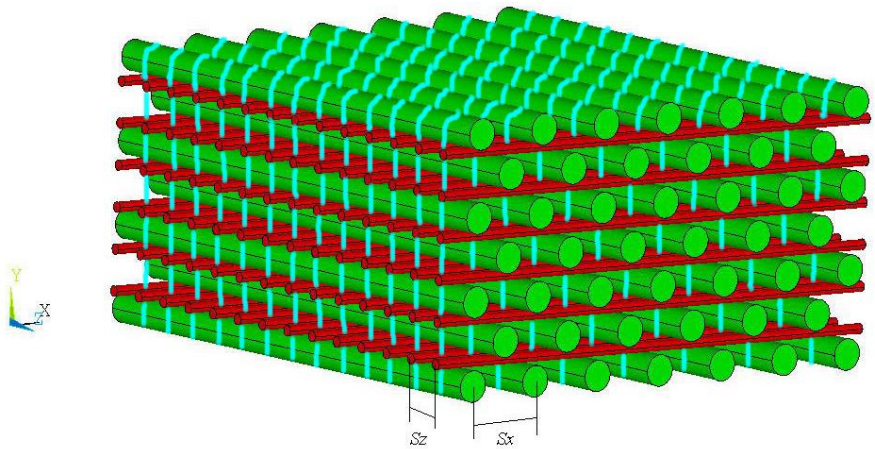

(c)

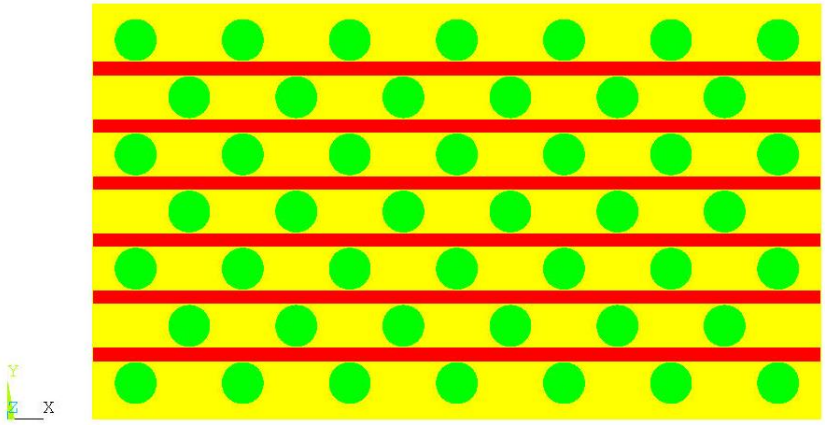

Figure1 Schematic diagram of 3D auxetic textile composite: (a) Auxetic textile composite made of four types of materials: the PU foam matrix (yellow), warp yarns (green), weft yarns (red) and stitch yarns (hidden in PU foam); (b) The sketch of auxetic textile reinforcements: warp yarns (green), weft yarns (red) and stitch yarns (cyan line); (c) The cross-section of the composite without showing stitch yarns in *XOY* plane.

All geometry parameters and material properties are listed in Table 1 and Table 2, respectively. In this composite, the matrix is soft open sell PU foam and its constitutive relation obeys the Ogden model. Because the stitch yarn is just used for fixing the warp and weft yarns during the fabrication process of the composite, the warp and weft yarns are the main bearing structural elements among these three types of yarns when the auxetic textile composite is compressed in *Y* direction. Therefore, this compression behavior is closely allied to the mechanical properties of warp and weft yarns for a given structure. In order to facilitate the analysis, the warp and weft yarn is assumed as transversely isotropic. The secant modulus (E_x) of uniaxial tension constitutive relations is used as their axial modulus, respectively. The radial modulus is assumed as one-fifteenth of the axial modulus [16]. The Poisson's ratio of the warp yarn and weft yarn is 0.2. In this work, the parameters listed in Table 1 and Table 2

are used by theoretical calculation and FEM simulation as a reference.

Table1 The geometry parameters of 3D auxetic textile structure and composite

Warp yarn			Weft yarn			Composite		
D_1(mm)	S_x(mm)	N_0	D_2(mm)	S_y(mm)	N_1	X (mm)	Y (mm)	Z (mm)
6	15	46	2	7.5	84	102	58	105.5

Table 2 The mechanical properties of constituent materials

Warp yarn		Weft yarn		PU foam					
E_x(MPa)	υ	E_x(MPa)	υ	μ_1(kPa)	μ_2(kPa)	α_1	α_2	β_1	β_2
30	0.2	30	0.2	2.4	1.75	19.8	19.7	1.4×10^{-3}	6.6×10^{-4}

2.2 Theoretical analysis of 3D orthogonal textile structure

(a)

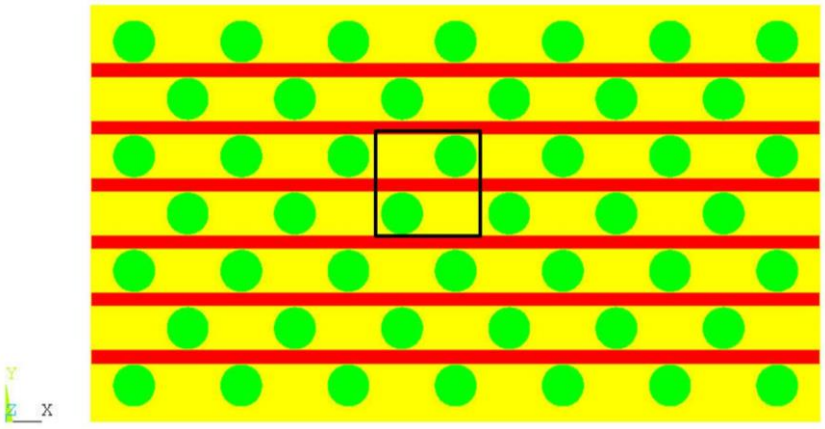

(b)

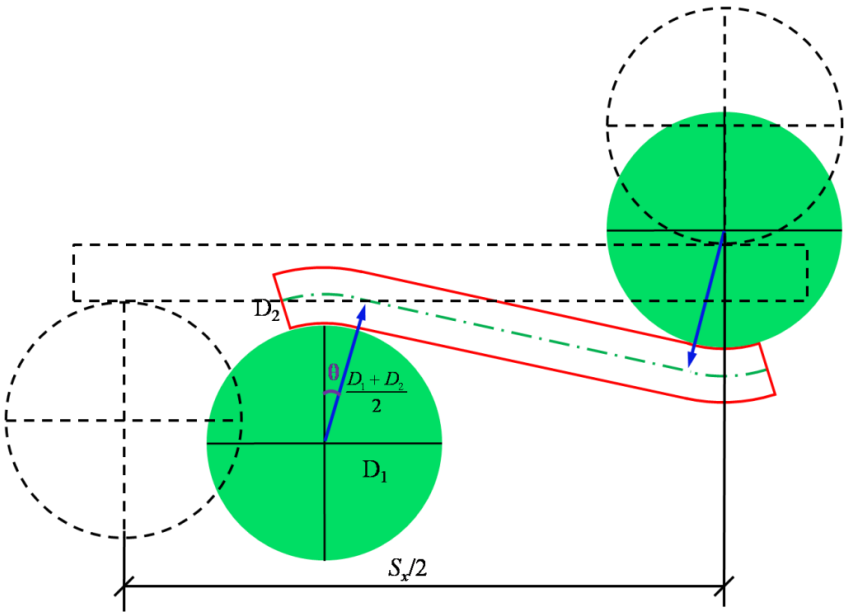

Figure 2 The FEM and theoretical model for 3D auxetic textile composite:(a) the FEM; (b) the sketch of compressed warp and weft yarn marked by dark square in (a), the dark dash lines are the undeformed edge of warp and weft yarns at the initial state. The deformed weft yarn is regarded as two arcs linked by a straight line. The central line (green dash line) is used to calculate the Poisson's ratio. Note: the warp and weft yarns are just for demonstration (not in scale).

For uniaxial loading on composite, a brief discussion on the deformation behavior under tension or compression in X and Y direction seems to be necessary at the beginning. For tension loading in X direction, the weft yarns are stretched and the composite deforms the same as a stiffer matrix. For tension loading in Y direction, the warp and weft yarns are separated from contact with each other after the stitch yarns are broken, which claims that the composite deforms like a tensile foam matrix. Similar deformation mechanism is observed when the composite is compressed in X direction, because the weft yarns cannot bear the compression loading. Different from the above three cases, the weft yarns get crimped when the composite is compressed in Y direction and the negative Poisson's ratio effect is obtained. In fact, this type of auxetic composite is developed to bear the compression loads in the composite thickness direction. Therefore, only the compression behavior of composite in Y direction is investigated in this work. The FEM of 3D auxetic textile composite and the theoretical model for the calculation of Poisson's ratio are shown Fig. 2a and 2b show, respectively. As the negative Poisson's ratio effect will become less significant when the PU foam is hard to be compressed, the matrix should be soft and compressible to obtain obvious negative Poisson's ratio effect. When the PU foam is soft enough, the Poisson's ratio of composites can be calculated from Fig. 2b. For

simplification, the following assumptions are adopted to conduct the theoretical analysis of the 3D auxetic textile composite.

1) The diameters of warp and weft yarn are kept unchanged during the compression;

2) The length of weft yarn is not increased under compression;

3) No void spaces exist at the contact points among the warp and weft yarns;

4) Warp and weft yarns are well bound by the PU foam matrix;

5) The PU foam is hyper elastic, very soft and compressible.

Based on these assumptions, the compression strain ε_y and its induced strain ε_x in horizontal direction can be calculated by Eq.1. In this equation, ε_y and ε_x are as a function of θ whose unit is radian as shown in Fig. 2b.

$$\begin{aligned} \varepsilon_y &= 1-\cos\theta-\theta\sin\theta+\frac{S_x\sin\theta}{2(D_1+D_2)} \\ \varepsilon_x &= 1-\cos\theta-\frac{2(D_1+D_2)(\sin\theta-\theta\cos\theta)}{S_x} \end{aligned} \tag{1}$$

For the convenience of description, the strains are positive in Eq.1. Introducing two dimensionless aspect ratios, $\xi_1=S_x/D_1$ and $\xi_2=D_2/D_1$, the Poisson's ratio v_{xy} can be calculated according to Eq.2.

$$v_{xy}=-\frac{\varepsilon_x}{\varepsilon_y}=-\frac{\xi_1(1-\cos\theta)-2(1+\xi_2)(\sin\theta-\theta\cos\theta)}{\xi_1\sin\theta+2(1+\xi_2)(1-\cos\theta-\theta\sin\theta)}\times\frac{2(1+\xi_2)}{\xi_1} \tag{2}$$

As θ is only an intermediate variable and the value of compression strain ε_y can directly obtained from the test, an explicit expression of the Poisson's ratio v_{xy} as a function of compression strain ε_y is more convenient for the practical use. Therefore, a

further derivation is conducted by replacing θ with ε_y in order to facilitate the calculation of v_{xy}. Since the cross section of the warp yarn is kept unchanged during the compression, it is obvious that θ decreases with the increasing of S_x and D_2. As the limitation of fabrication, the minimum value of S_x is twice of the diameter of warp yarn D_1. The maximum value of θ can be calculated by Eq. 3 when $S_x=2D_1$ (or $\xi_1=2$)

$$\theta = \min\left\{\frac{1}{1+\xi_2}, \arccos\frac{1+2\xi_2}{2(1+\xi_2)}\right\} \tag{3}$$

From Eq. 3, we can find that the maximum value of θ is 1. Taking $\xi_2=0.1$ for example, $\theta_{max}=0.91$ and considering the continuity and symmetry of weft yarn, the straight part of weft yarn is in the tangential direction of contact point under compression as shown in Fig. 2b. To simplify the expression of Poisson's ratio and strains, sine and cosine functions are approximated by Taylor's polynomial. We can get

$$\sin\theta = \theta,\ \cos\theta = 1-\frac{\theta^2}{2} \tag{4}$$

Obviously, only when θ is less than 0.5, the overestimation of $\sin\theta$ is not more than 5% by θ. In our case, θ is less than 1. Thus the maximum overestimation is about 19%. But this is just for some extreme cases and its induced variation on Poisson's ratio will be carefully assessed in the following verification section. Based on this, the relation between ε_y and θ can be expressed by a quadratic equation as shown in Eq. 5.

$$\theta^2 - \frac{\xi_1}{1+\xi_2}\theta + 2\varepsilon_y = 0 \tag{5}$$

From Eq. 5, we can get

$$\varepsilon_y \le \frac{N^2}{8} \tag{6a}$$

$$\theta = \frac{N - \sqrt{N^2 - 8\varepsilon_y}}{2} \tag{6b}$$

Where $N = \frac{\xi_1}{1+\xi_2}$.

From Eq. 6a and combined with the deformation mechanism, we can find that the maximum ε_y can be determined by the minimum values of the following

$$\varepsilon_y = \min\left\{\frac{\xi_1^2}{8(1+\xi_2)^2}, \frac{1}{2(1+\xi_2)}\right\} \tag{7}$$

Obviously, the maximum compression strain is less than 0.5 and determined by aspect ratios ξ_1 and ξ_2 because the diameter of weft yarn could not be reduced to zero. Substituting the Eq. 6b into Eq. 3, we can get

$$\nu_{xy} = \frac{M(M-1)}{M+1}, \quad M = \sqrt{1 - \frac{8\varepsilon_y}{N^2}} = \sqrt{1 - \frac{8\varepsilon_y(1+\xi_2)^2}{\xi_1^2}} \tag{8}$$

To further simplify the above equation, M can be approximated by using the Maclaurin series for the sum of first 3 terms as shown in Eq. 9.

$$M = 1 - \frac{4}{N^2}\varepsilon_y - \frac{16}{N^4}\varepsilon_y^2 \tag{9}$$

Then, substituting Eq. 9 into Eq. 8, ν_{xy} can be expressed as a function of ε_y.

$$\nu_{xy} = -1 - \frac{4}{N^2}\varepsilon_y - \frac{16}{N^4}\varepsilon_y^2 + \frac{1}{1 - \frac{2}{N^2}\varepsilon_y - \frac{8}{N^4}\varepsilon_y^2}, \quad N = \frac{\xi_1}{1+\xi_2} \tag{10}$$

Using the sum of first 3 terms of Maclaurin series again, we can get

$$\nu_{xy} = -\frac{2}{N^2}\varepsilon_y - \frac{4}{N^4}\varepsilon_y^2 = -\frac{2(1+\xi_2)^2}{\xi_1^2}\varepsilon_y - \frac{4(1+\xi_2)^4}{\xi_1^4}\varepsilon_y^2 \quad (11)$$

Therefore, an explicit expression of ν_{xy} as a function of ε_y is obtained. Eq. 11 clearly shows the relationship of ν_{xy} with ξ_1 and ξ_2 and ε_y.

(a)

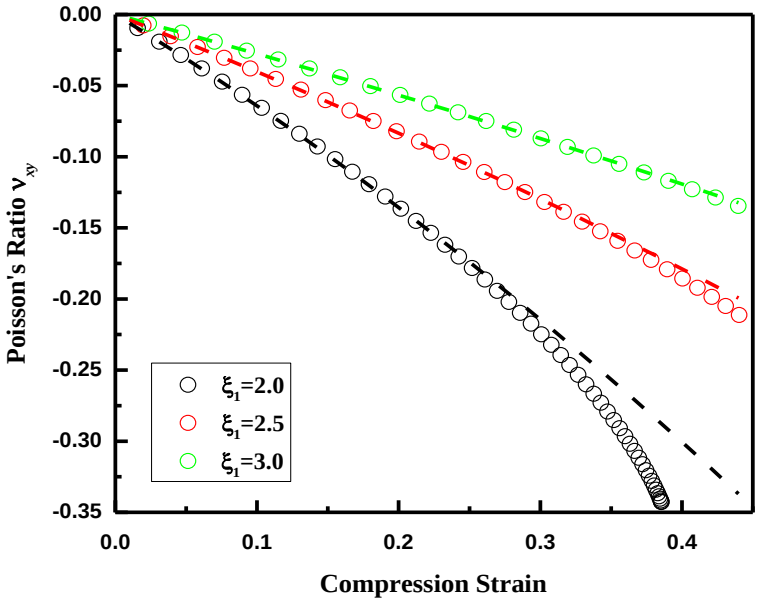

(b)

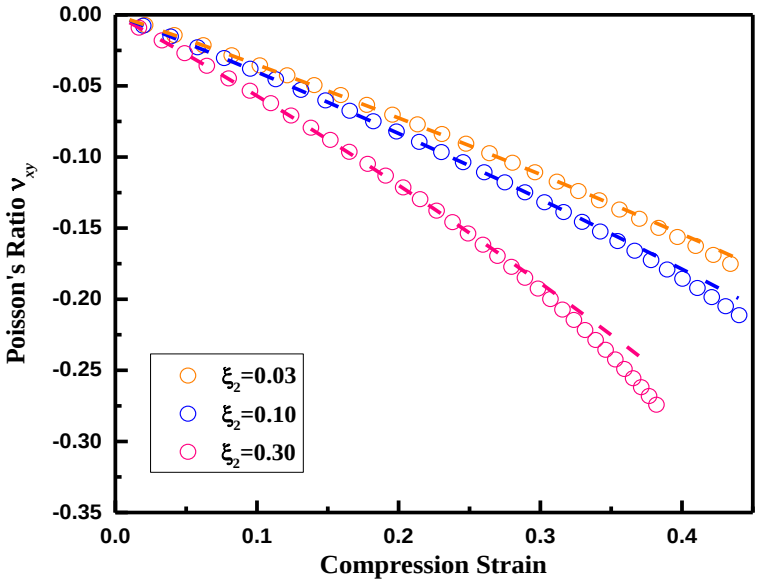

Figure 3 Poisson's ratio values as a function of ε_y calculated from Eq. 2 (circle) and Eq.11(dash line): (a) when ξ_2 =0.1; (b) when ξ_1 =2.5.

A comparison of the Poisson's ratio values calculated from Eq. 2 and Eq.11 for different ξ_1 and ξ_2 are shown in Fig. 3. From Eq. 3a, we can find that Eq.11 is the overestimation of Eq. 2 when ξ_2=0.1 and the difference increases with the deceasing of ξ_1. The effect of ξ_2 on the calculation of Poisson's ratio is illustrated in Fig.3b by setting ξ_1=2.5. It is clear shown that the difference between Eq. 2 and Eq. 11 increases with the increasing of ξ_2 and it is reasonable for this simplification when ξ_2 is not more than 0.1.

2.3 Uniaxial compression test

To study the negative Poisson's effect of 3D auxetic textile composite under uniaxial compression, the composite was compressed by an Instron 5566 Universal Testing Machine using a 10kN load cell in ambient. The compression was conducted by a displacement control function with a rate of 40mm/min. A High-resolution CMOS camera was fixed in front of the sample to take a picture per every two seconds. To calculate the experimental strain and Poisson's ratio, four warp yarns were marked on the composite as shown in Fig.4. Before the compression, the original distance between the central points of marked warp yarns A and B was measured as reference. Then the distance between the central points of warp yarns A and B was measured from each image captured by camera during compression. Based on the distances measured from the images before and during compression, the contract strain in *X* direction ε_x could be calculated. In the same way, the compression strain ε_y could be

also calculated from the measured distances between the marked warp yarn C and D.

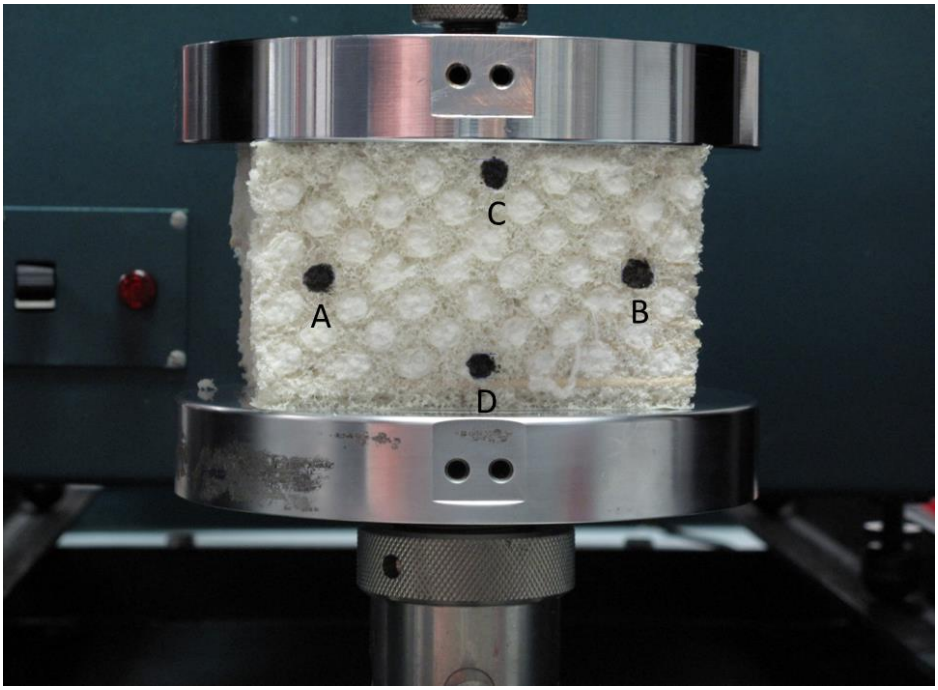

Figure 4 The uniaxial compression test of 3D auxetic textile composite conducted with an Instron 5566 Universal Testing Machine. Four warp yarns marked with black color are used to record the deformation of the composite during the compression.

2.4 Finite element analysis

The presented work is initiated to better estimate the Poisson's ratio of 3D auxetic textile structure under uniaxial compression. It is the best approach to simulate the compression behavior by using the finite element method. The mechanism of negative Poisson's ratio effect of the composite is the inward movement of warp yarns due to crimping of weft yarns. From this point of view, if the spaces among weft yarns are small enough, the 3D auxetic textile structure can be simplified as a plane strain model by equivalent stiffness reduction of the weft yarn. For the convenience of investigation, the FEM is modeled by ANSYS Parameter Design Language (APDL)

and all geometrical parameters and mechanical properties of constituent materials are selected as modeling parameters. The software used is ANSYS 11.0 and the element used is PLANE182. Taking the geometrical dimensions and mechanical properties of constituent materials listed in Table 1 and Table 2 as an example, the procedure of modeling and meshing are presented in Fig. 5.

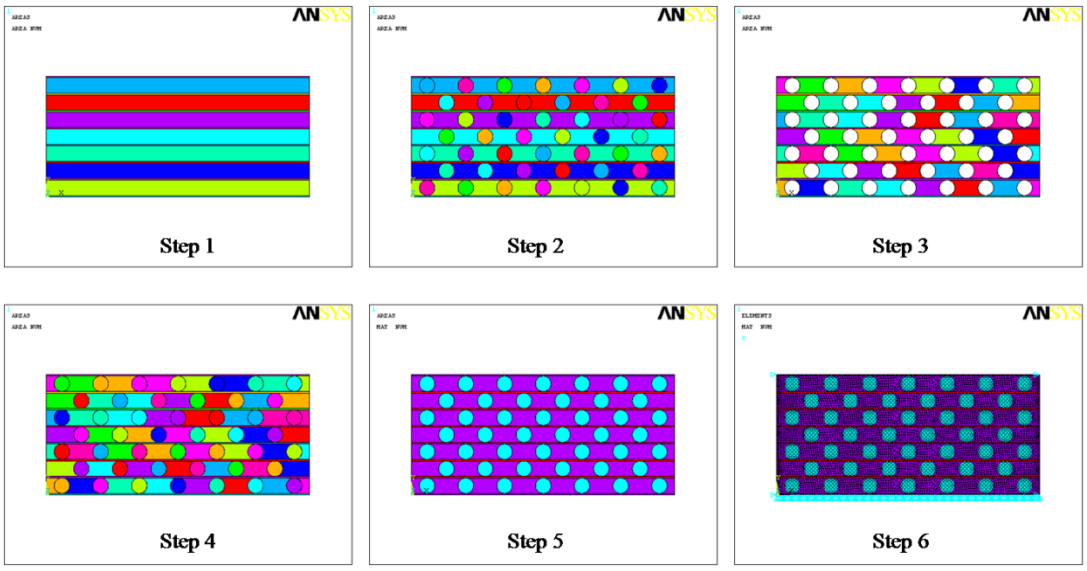

Figure5 The procedure of creating a FEM. In steps 1, 2, 3 and 4, the areas are numbered by color. In step 5, three colors are used to number the warp yarn (cyan), weft yarn (red) and PU foam (purple), respectively. The boundary condition and element shape are shown in Step 6. But the elements shown in Step 6 are just for demonstration and not for simulation.

As shown in Fig.5, all the procedure includes the six steps. In the first step, 15 areas, which are numbered from A1 to A15 in sequence, are created using 32 key points from the bottom to the top by one after another. Among these areas, the weft yarns are A3, A5, A7, A9, A11 and A13. The rest of areas are PU foam matrix and grouped into a component PUF matrix. As the numbers of warp yarns between two adjacent weft yarn layers are different, their areas are named as odd layers (A2, A6, A10 and A14)

and even layers (A4, A8 and A12) to facilitate the description without any physical meaning. In the second step, the cross-sections of warp yarns are created in odd layers and even layers, respectively. All warp yarns are grouped into a component WARP_YARN. In the third step, the WARP_YARN is subtracted from PUF matrix and deleted after subtraction. After that, the geometric model of PU foam matrix is created. In the fourth step, the warp yarns are generated by the previously resulting lines by the operation of subtraction. Till now, the geometric model of the textile structure is created. In the fifth step, all areas are associated with related mechanical properties of constituent materials and element attributes. The warp and weft yarns are meshed by mapping and the PU foam is freely meshed to generate the FEM. For the warp yarn, as the cross sections of the warp yarns is the isotropic plane, its radial modulus is assumed to be equal to its Young's modulus. However, for the weft yarn, its mechanical property is modeled as transversely isotropic by assuming that its orthotropic moduli E_y and E_z are the same. For the hyperelastic compressible PU foam, the 2-parameter OGDEN (foam) is used to characterize it. In the sixth step, the boundary condition and displacement load are applied. For the boundary condition, the nodes in the bottom line are fixed in Y direction and the nodes in the top are coupled together in Y direction. For the condition of no slippage between the compression plates and composite sample, four nodes in the corners of this plane model are fixed in X direction. If there are no friction between the compression plates and sample and the sample can shrink, only the nodes located in middle of the model are fixed in X direction (not shown in Fig. 5). The displacement load is applied to one

node located in the top of FEM to simulate the uniaxial compression. When the FEM is established, the nonlinear solution including large-deflection effect in a static analysis is solved without automatic load stepping and a predictor is activated. In this work, the full Newton-Raphson is used to solve the nonlinear equations. Because there are no contact elements in this model, the time of solving is greatly reduced and the convergence of solution becomes much easier.

Similar to the experimental measurement of Poisson's ratio, the warp yarns are numbered to calculate the Poisson's ratio in FEM simulation as shown in Fig. 6. It is obvious that the Poisson's ratio will be different by different pair of warp yarns due to the edge effect. To systematically investigate the variety of Poisson's ratio, 21 strains ε_x in X axis are selected to calculate the Poisson's ratio, while the strain ε_y in Y axis is only calculated using the displacement divided by the length of composite in Y direction, as the deformation of the composite in Y direction is directly controlled by the compression plates and the edge effect on the calculation of ε_y is not evident. Consequently, all strains and Poisson's ratios to be calculated are defined by Eq.12.

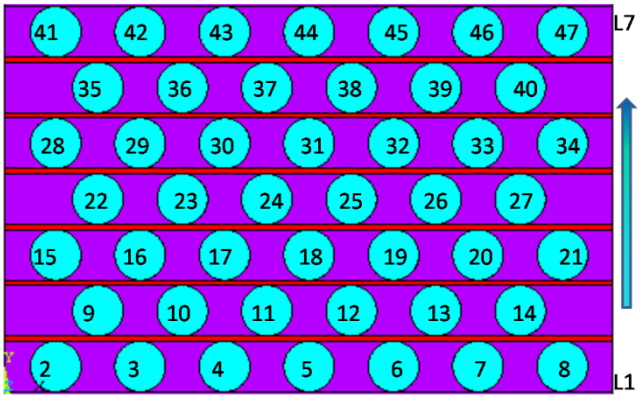

Figure 6 The sketch for serial number of warp yarns. The warp yarns are numbered from 2 to 47 for the calculation of Poisson's ratio. In order to describe the strain and Poisson's ratio conveniently, the warp

yarn layers are also numbered from bottom to top by L1 to L7.

$$\varepsilon_{jk} = \frac{U_{x,a} - U_{x,b}}{X_{ab}} \quad (j = 1, 2\cdots 7; k = 1, 2, 3)$$
$$\varepsilon_y = \frac{U_y}{Y} \tag{12}$$
$$\nu_{jk} = -\frac{\varepsilon_{jk}}{\varepsilon_y} \quad (j = 1, 2\cdots 7; k = 1, 2, 3)$$

In Eq. 12, the subscript x and y stand for the direction of displacement, j is the number of layer and k is the serial number of strain and Poisson's ratio. The subscript a and b are the serial number of warp yarn running from 2 to 47. U_x and U_y are the displacements in X and Y direction when compressed in Y direction. X_{ab} is the horizontal distance between a_{th} and b_{th} warp yarns before compression. Y is the original length of the composite in Y direction. All calculated strains and their related warp yarns are defined and listed in Table 3. The numeration of Poisson's ratio is the same as strain in X direction and is not listed here for brevity.

Table 3 Definition of strain in X direction for each layer

No. Layer	No. b	No. a	Strain	No. Layer	No. b	No. a	Strain
1	2	8	ε_{11}	2	9	14	ε_{21}
	3	7	ε_{12}		10	13	ε_{22}
	4	6	ε_{13}		11	12	ε_{23}
3	15	21	ε_{31}	4	22	27	ε_{41}
	16	20	ε_{32}		23	26	ε_{42}
	17	19	ε_{33}		24	25	ε_{43}
5	28	34	ε_{51}	6	35	40	ε_{61}
	29	33	ε_{52}		36	39	ε_{62}
	30	32	ε_{53}		37	38	ε_{63}
7	41	47	ε_{71}				
	42	46	ε_{72}				
	43	45	ε_{73}				

3. Results and discussion

As the negative Poisson's ratio effect only appears in *XOY* plane when the 3D auxetic textile composite is compressed in *Y* direction, only the Poisson's ratio v_{xy} is calculated in this work to investigate the auxetic behavior of 3D textile composite under uniaxial compression. In the other two planes, as there is no negative Poisson's ratio effect under compression, their Poisson's ratios will not be calculated.

3.1 Effects of boundary conditions

To simulate the mechanical behavior of auxetic textile structural composite under uniaxial compression, the friction between the compression plates and composite sample must be considered. Therefore, two extreme conditions are studied by FEM simulation. Case one is that the friction between the compression plates and the sample is large enough to make sure that no slippage occurs during compression, which is corresponding to the fixed four corners of the sample in *X* direction. The other case is no friction between the compression plates and composite sample and is simulated by only fixing the center of sample in *X* direction. All calculated Poisson's ratios by FEM for these two cases with the same structure are shown in Fig.7.

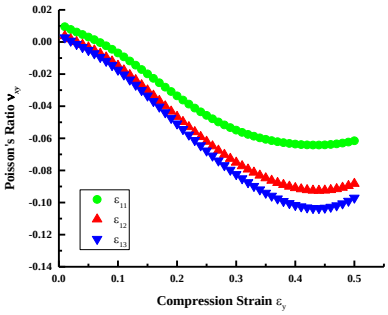

(a1)

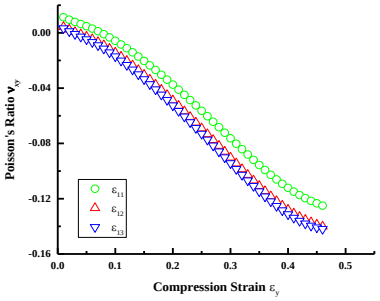

(a2)

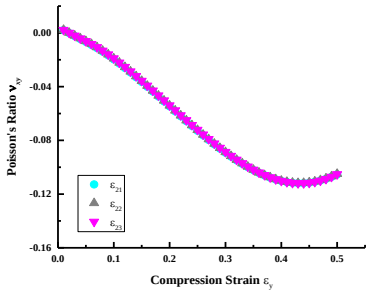

(b1)

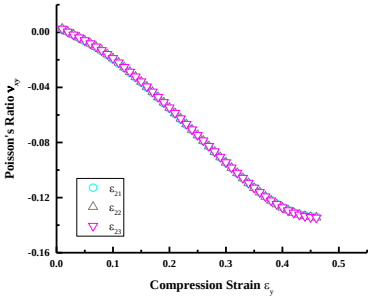

(b2)

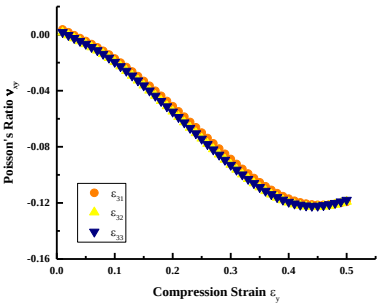

(c1)

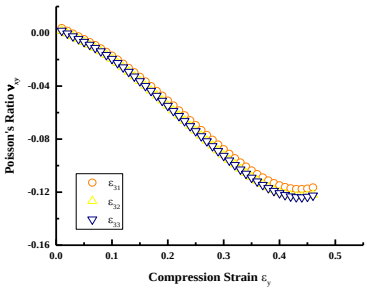

(c2)

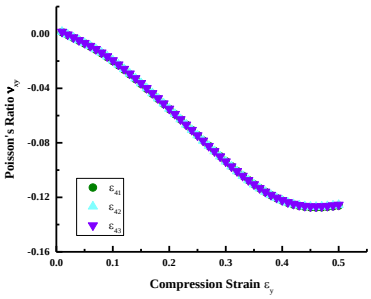

(d1)

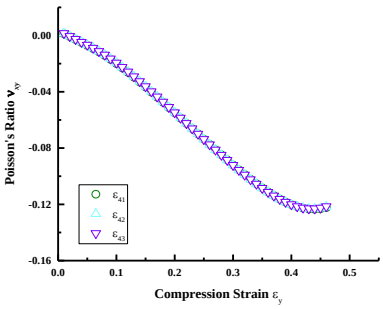

(d2)

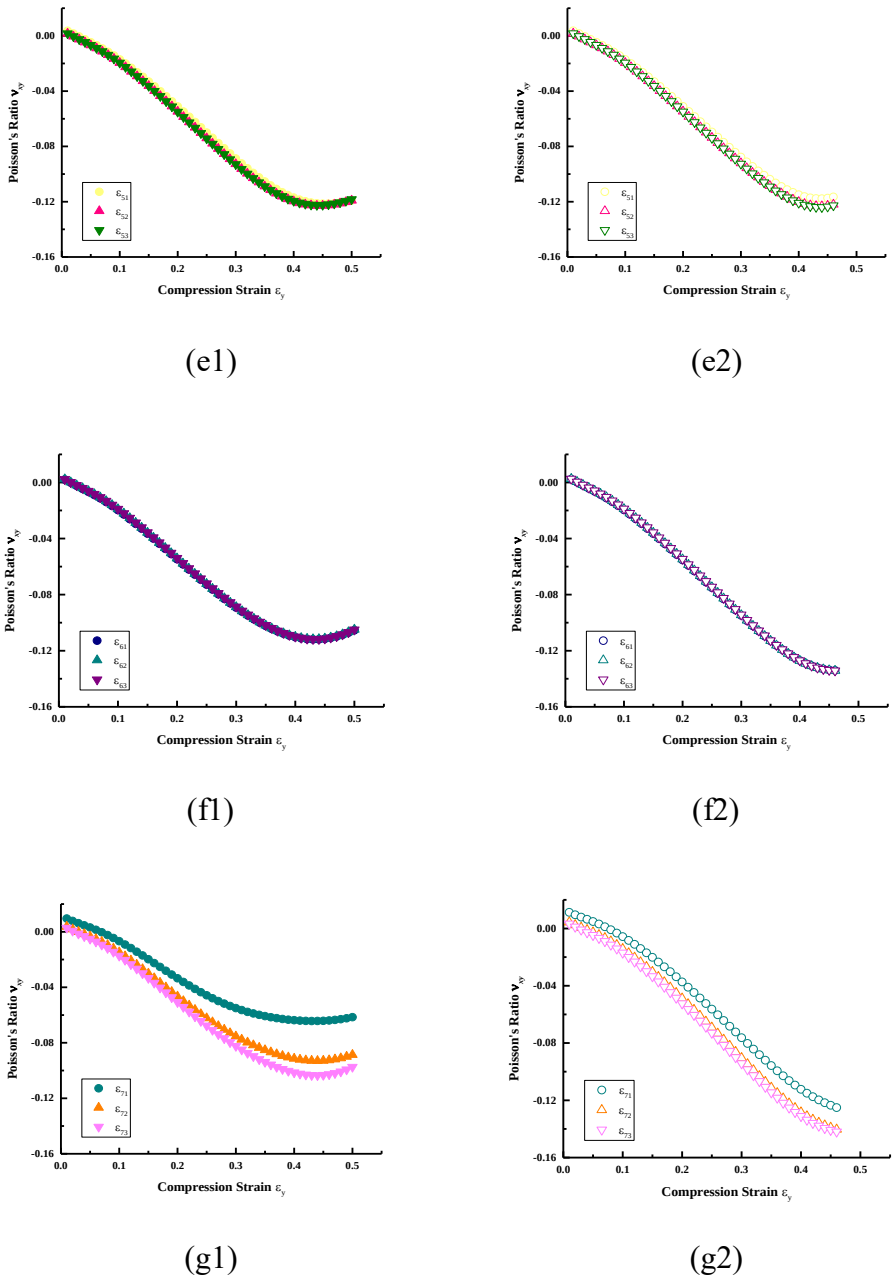

Figure 7 The Poisson's ratios calculated from FEM for two cases: no slippage (solid) and no friction (open). (a)-(g) is for layer 1 to 7. Left column (a1)-(g1) is for the case of no slippage and the right column (a2)-(g2) is for no friction.

For the case of no slippage, the negative Poisson's ratio effect in L1 and L7 are much smaller than the rest, because the contraction of L1 and L7 is reduced in *X* direction due to the existence of friction between the plates and sample. Especially, the

Poisson's ratios calculated by the outer warp yarns are about -0.065 in these two layers, when the compression strain is more than 0.45. For the case of no friction, because there is no constrain in the top and bottom layers, the negative Poisson's ratio effects in L1, L2, L6 and L7 are slightly larger than the others and reach to -0.140. For both cases, we can found that all the Poisson's ratios calculated by warp yarns located in L3, L4 and L5 are close to -0.127. In order to clearly show the difference of Poisson's ratio obtained at L4 for two cases, the averaged Poisson's ratios are illustrated in Fig.8. When the compression strain is less than 0.25, the results for two boundary conditions are exactly the same. However, the negative Poisson's ratio effect obtained for no slippage case is slightly larger than that for no friction case when the compression strain exceeds 0.25. The reason for this difference is that the deformation is lager in the outer layers (L1 and L7) for no friction case. For this reason, we suggest to use the average of calculated Poisson's ratio by warp yarns in the middle layer L4 as the characteristic value of the composite. Thus, the calculated Poisson's ratios in L3, L4 and L5 are nearly not affected by boundary conditions and the FEM is sufficient to characterize the negative Poisson's ratio effect of 3D textile composite. To save the solving time of FEM simulation, this FEM is used to investigate the effect of aspect ratios and material properties on negative Poisson's ratio effect of 3D auxetic textile composite. For the boundary condition, 'no slippage' is used to calculate the Poisson's ratio in this work.

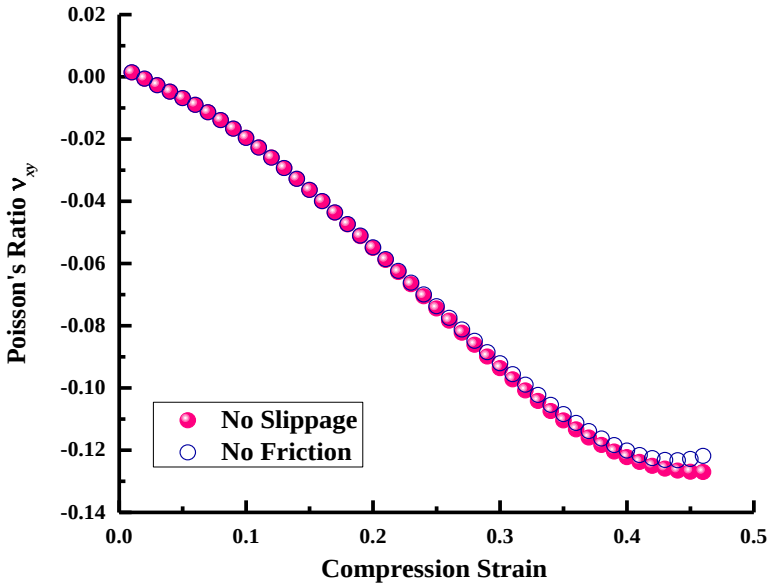

Figure 8 The relation between the averaged Poisson's ratio calculated from the warp yarns in layer 4 and compression strain for two boundary conditions: no slippage (pink sphere) and no friction (royal open circle).

3.2 Validation of FEM simulations

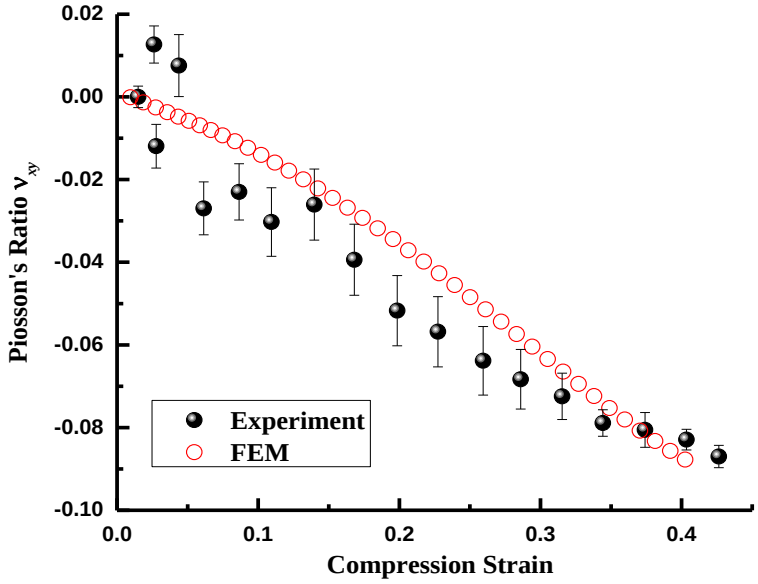

Figure 9 Comparison of Poisson's ratio between the FEM simulation (red open circle) and experimental results (black solid sphere).

To check the accuracy of FEM simulation, the simulation results are shown in Fig. 9 with the experimental data. Obviously, the simulation results are close to the experimental data. When the compression strain is less than 0.3, the difference between the simulation and experimental data is slightly larger than the rest. The main reason may be no consideration on the curvature of weft yarns at the initial state. As can be seen from Fig. 9, the Poisson's ratio rapidly drops with the increasing of compression strain for both experimental data and calculation results. Accordingly, the FEM is valid to predict the Poisson's ratio of 3D auxetic textile composites.

3.3 Comparison between the theoretical analysis and FEM simulation

To verify the accuracy of Eq.11, the FEM is used to simulate the mechanical behavior of the composite under compression. To make sure that the deformation of warp yarns can be ignored compared with the deformation of weft yarns, the Young's modulus of warp yarns is set as 10GPa for the FEM simulation, which is much larger than that of weft yarn. The diameters of warp and weft yarns are 6mm and 0.6mm, respectively. The aspect ratio ξ_1 is ranged from 2 to 5. The simulation results and theoretical analysis are shown in Fig. 10a. The figure reveals that the calculated Poisson's ratio by Eq.11 is getting closer to the simulation results with the increasing of aspect ratio ξ_1. For the case when aspect ratio ξ_1=2, the difference between the simulation results and theoretical analysis is induced by the underestimation of $\sin\theta$. But the increasing

rate of compression strain decreases when the intermediate variable θ becomes larger. Therefore, the difference between the Eq.11 and simulation becomes smaller when the compression strain is getting larger.

(a)

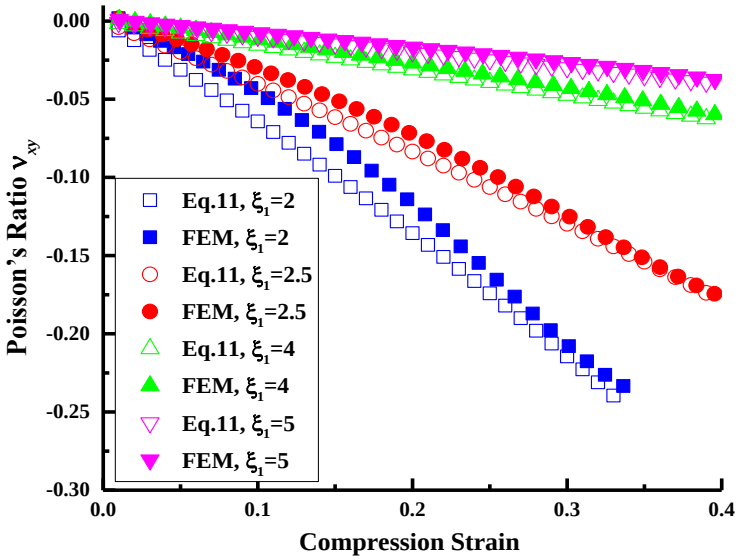

(b)

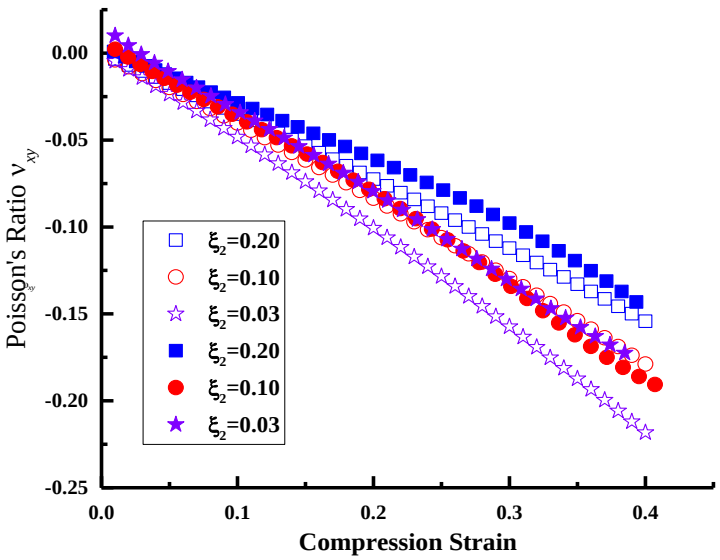

Figure 10 Comparison between the theoretical calculation (open symbol) and FEM simulation (solid symbol): (a) for different aspect ratio ξ_1 and (b) for different aspect ratio ξ_2.

To investigate the effect of aspect ratio ξ_2, three cases are shown in Fig.10b when ξ_2 changes from 0.20 to 0.03. It is suggested that Eq. 11 is suitable for calculating the Poisson's ratio when ξ_2=0.1. The cause of difference between the theoretical calculation and FEM simulation is the underestimation of the compression and extension of weft yarn in the theoretical calculation. It is clear that the compression strain of the composite in Y direction contains two parts: bending and compression of weft yarns. With the increasing of aspect ratio ξ_2, the compression of weft yarn in Y direction is also increased. Therefore, the compression strain is underestimated by the theoretical analysis and the negative Poisson's ratio effect is overestimated. For ξ_2=0.03, because of the existence of PU foam, the radius of arc is underestimated by the theoretical analysis, which is the main reason for the overestimation of negative Poisson's ratio effect.

3.4 Effects of aspect ratio ($\xi_1$and ξ_2)

In the theoretical analysis, the cross section of warp yarn is assumed to be unchanged during compression. Therefore, the Young's modulus of warp yarns is set at a high value (10 GPa) for the FEM in order to compare with the theoretical calculation results. The material properties of the weft yarn and PU foam used are the same as listed in Table 2. As shown in Fig.11, for a given aspect ratio ξ1=2.5 and ξ2=0.1, the Poisson's ratios obtained by FEM simulation for 4mm and 6mm warp yarn are the same and have a close agreement with the theoretical calculation results. This confirms that the Poisson's ratio is not determined by the diameter of warp or weft yarn individually.

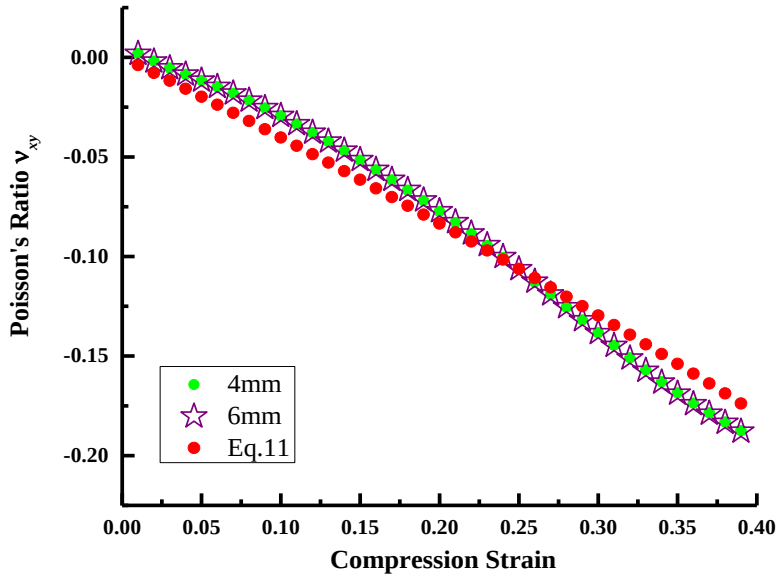

Figure 11 The Poisson's ratios calculated from Eq.11 and FEM simulation for the composites made with different warp yarn diameters by fixing ξ_1=2.5 and ξ_2=0.1.

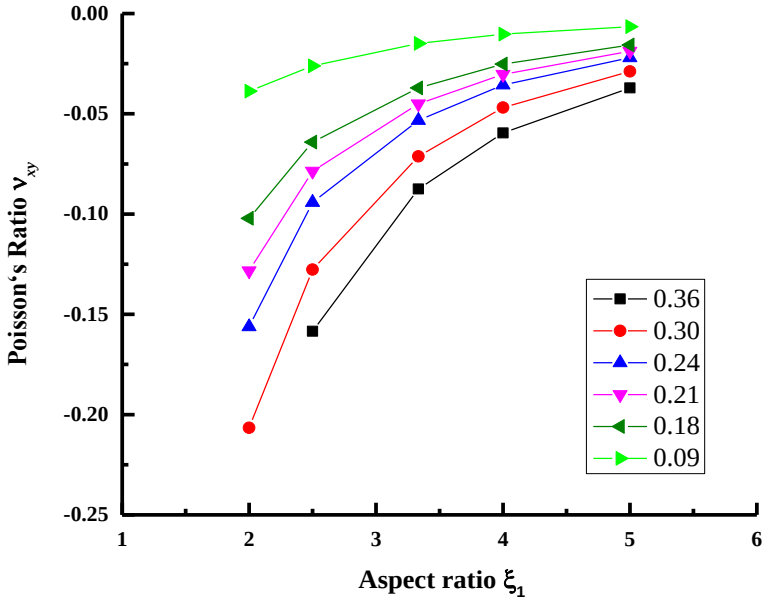

Figure 12 The Poisson's ratio as a function of aspect ratio ξ_1 under different compression strain from 0.09 to 0.36.

Because the negative Poisson's ratio is produced by the crimping of weft yarns, the warp yarn spacing plays a vital role in the generation of negative Poisson's ratio effect. As a result of the fabrication, the minimum of warp yarn spacing is twice of the diameter of warp yarn (ξ_1 is not less than 2). Hence, in Fig. 12, the aspect ratio ξ_1 is ranged from 2 to 5 by fixing ξ_2=0.1. It is clearly shown that the negative Poisson's ratio effect decreases with the increase of aspect ratio ξ_1 for each compression strain ε_y and the maximum negative Poisson's ratio effect reaches to -0.23 when ξ_1=2 and ε_y=0.30. When the aspect ratio ξ_1 reaches to 5, the negative Poisson's ratio is around -0.02 for all aspect ratio ξ_1, which is nearly immeasurable. Therefore, the warp yarn spacing should not exceed five times of the diameter of warp yarn in order to generate remarkable negative Poisson's ratio effect.

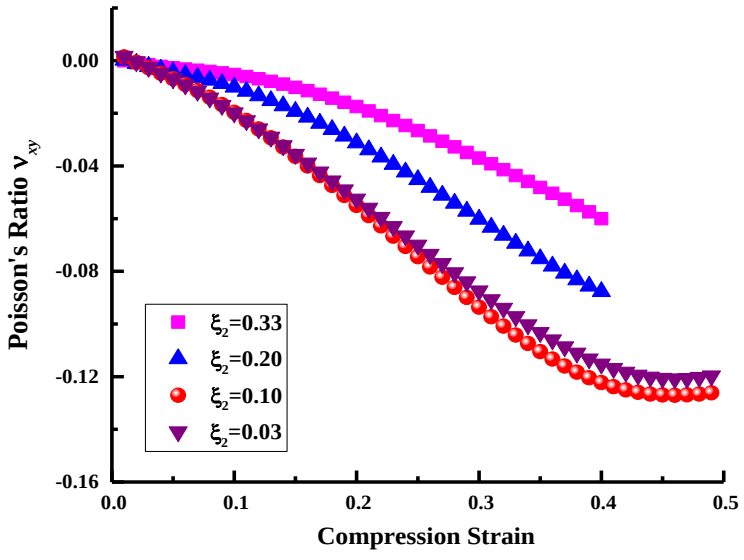

Figure 13 The effect of aspect ratio ξ_2 on negative Poisson's ratio effect of auxetic textile composite

To study the effect of aspect ratio ξ_2 on the negative Poisson's ratio effect of 3D

auxetic textile composite, the aspect ratio ξ_1 is set to 2.50. The same mechanical properties of constituent materials are listed in Table 2 are used. But the radial modulus of warp and weft yarns are 1/60 of E_x. The simulated Poisson's ratios by FEM under uniaxial compression for four different values of aspect ratio ξ_2 are shown in Fig. 13. From this figure, we can find that the negative Poisson's ratio effect increases with the decreasing of aspect ratio ξ_2 from 0.33 to 0.10, but slightly decreases from 0.10 to 0.03. Therefore, for these four cases, the maximal negative Poisson's ratio is -0.13 for this composite.

3.5 Effects of material properties

In the theoretical analysis, there is no consideration on the mechanical properties of composite components. But the negative Poisson's ratio effect can also be affected by the material properties of composite components: reinforcement and matrix. In 1992, the effect of matrix properties on the negative Poisson's ratio effect had been investigated by Evans and Nkansah[19] using a two-dimensional FEM of a reentrant network composite. They found that the negative Poisson's ratio effect was reduced if the stiffness of the matrix was sufficiently high to swamp the flexural expansion of the fiber network. Thus the Poisson's ratio is only negative above certain modulus values of the fiber. Similar to this reentrant network composite, the Poisson's ratio of 3D auxetic textile composite is also reduced for the stiffer matrix. So, in this work, only the yarn properties effects are studied. For the deformations of warp and weft yarns, the cross section of warp yarn may be changed from a circle to an ellipse and the weft yarn can be stretched under compression. In this section, the effects of

mechanical properties of the warp and weft yarns are investigated by FEM simulation. In order to facilitate the description of their deformations, the normalized Young's modulus E^* is defined as the ratio of warp yarn to weft yarn, e.g. $E^*=E_{warp}/E_{weft}$. For facilitating the analysis, the values of ξ_1 and ξ_2 are fixed as 2.5 and 0.1, respectively. The Young's modulus of weft yarn is 30MPa in the axial direction and 0.5MPa in the radial direction. Changing only the Young's modulus of the warp yarn, the Poisson's ratios obtained by FEM simulation are shown in Fig.14a. From this figure, we can find that the negative Poisson's ratio effect increases with the increasing of E^*. The decreasing of negative Poisson's ratio effect is caused by the cross sectional deformation of warp yarn, and the negative Poisson's ratio effect obtained by rigid warp yarn is larger than the deformable one. To investigate the influence of warp yarn deformation on the negative Poisson's effect, the compression strain in the diameter of warp yarn in Y direction is obtained and illustrated in Fig.14b. From this figure, we can see that the compression strain of warp yarn increases with the decreasing of its Young's modulus. However, when the normalized Young's modulus exceeds 4, the cross sectional deformation of warp yarn can be ignored (the maximum strain is not more than 0.03) during compression. For composite with nearly undeformed warp yarn (E^*=20000), the maximum negative Poisson's ratio reaches to -0.19. Based on this, to obtain maximum negative Poisson's ratio effect, the warp yarn should be much more rigid than the weft yarn.

(a)

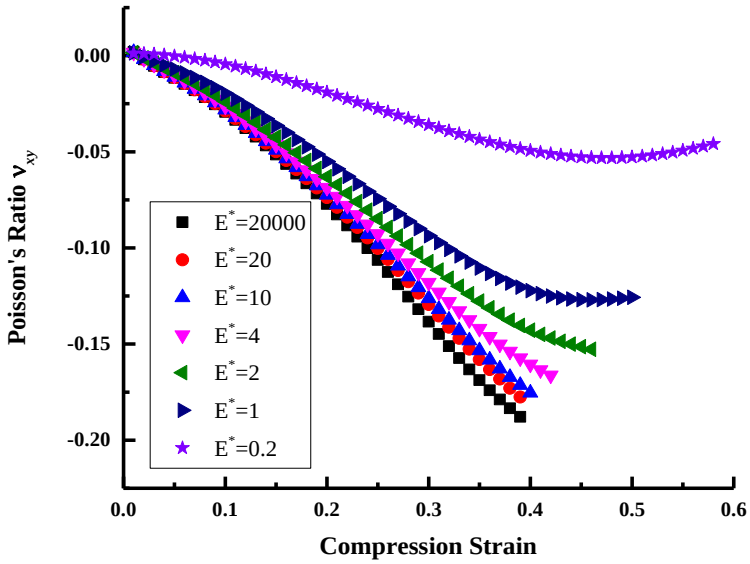

(b)

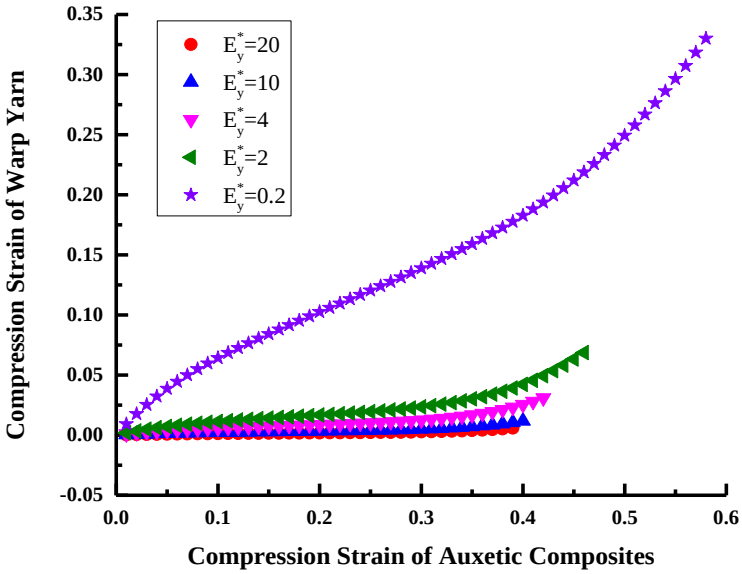

Figure 14 The effect of E^* on negative Poisson's ratio effect: (a) the relation of Poisson's ratio and compression strain; (b) the relation of compression strains of warp yarn and composites.

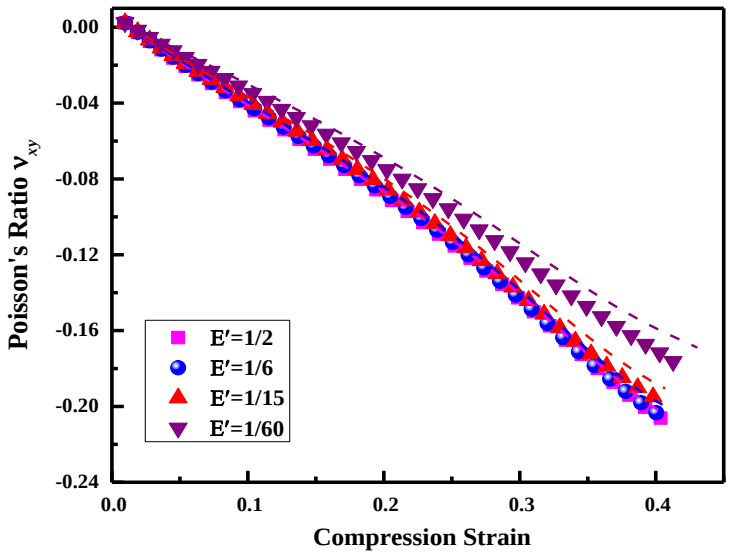

Figure 15 The effect of E′ on the Poisson's ratio. The dash line is directly obtained by FEM simulation and the sphere is calculated from the corresponding dash line by subtracting the compression of weft yarn.

Besides of the above effects, the negative Poisson's ratio effect of the auxetic composite is also affected by the compression and stretching of weft yarn. Fixing the radial modulus E_r to 0.5Mpa, the ratio of the radial modulus E_r to the axial modulus E_x of weft yarn, $E' = E_r / E_x$, is defined to study this effect. As shown in Fig.15, the negative Poisson's ratio effect is reduced by the compression of weft yarn and this influence is reduced with the increasing of E′. From this figure, we can suggest that the negative Poisson's ratio effect is deceased with the deceasing of E′, but the difference is not very remarkable from 1/15 to 1/2. Hence, auxetic composites can be fabricated by numerous yarns.

4. Conclusions

Owning to the outstanding mechanical properties, auxetic composites have attracted

more attentions and plenty of new structures are fabricated. In this work, we study the negative Poisson's ratio effect of novel 3D auxetic orthogonal textile composites by theoretical analysis and 2D FEM simulation. Based on the above results and discussion, the following conclusions are obtained:

- A simple formula Eq.11 is derived for the theoretical calculation of the Poisson's ratio from the geometrical parameters and compression strain. Without considering the deformation of warp yarns and stretching of weft yarns, this formula overestimates the negative Poisson's ratio effect. Limited by the assumptions for simplification, Eq.11 is not suitable for the prediction of Poisson's ratio for some extreme cases. But it clearly shows that the negative Poisson's ratio effect is affected by two aspect ratios (ξ_1 and ξ_2) and compression strain rather than the individual diameter of warp yarn, diameter of weft yarn or warp yarn spacing.

- The Poisson's ratio obtained by 2D FEM is close to the experimental data, which means that the 2D FEM is valid to predict the Poisson's ratio of 3D auxetic composite.

- The negative Poisson's ratio effect obtained by 2D FEM simulation is slightly smaller than that of theoretical data. This is caused by the underestimation of compression strain without considering the compression deformation of weft yarn in the theoretical analysis. Because the deformation of warp and weft yarn plays a vital role in the negative Poisson's ratio effect, but is not included in the

theoretical analysis, the 2D FEM simulation is used to systematically study both effects of material mechanical properties and geometry parameters on negative Poisson's ratio effect of the composite.

- To obtain high negative Poisson's ratio effect, in the selection of materials, the warp yarns should be rigid and the weft yarn is not stretchable and compressible. In the selection of the geometry parameters, the aspect ratio ξ_1 is 2 and ξ_2 is around 0.1.

The negative Poisso ratio behavior of 3D auxetic textile composite under compression is well characterized by a simplified equation and a 2D FEM in this study. The outcomes of this work may shed a light on the investigation of auxetic composites. Because of the complexity of PU foam, we did not study its effect on the negative Poisson's ratio effect numerically. In fact, the auxetic structure has an advantage on bearing of impact loading. Their dynamic behavior can also be investigated in the same way as we have done in this work.

Acknowledgements

The authors would like to thank the funding support from the Research Grants Council of Hong Kong Special Administrative Region Government in the form of a GRF project (No. 515812).

References

1. R. Lakes, *FOAM STRUCTURES WITH A NEGATIVE POISSONS RATIO.* Science, 1987. **235**(4792): p. 1038-1040.

2. R. Lakes, *ADVANCES IN NEGATIVE POISSONS RATIO MATERIALS.* Advanced Materials, 1993. **5**(4): p. 293-296.

3. B.D. Caddock and K.E. Evans, *MICROPOROUS MATERIALS WITH NEGATIVE POISSON RATIOS .1. MICROSTRUCTURE AND MECHANICAL-PROPERTIES.* Journal of Physics D-Applied Physics, 1989. **22**(12): p. 1877-1882.

4. K.E. Evans and B.D. Caddock, *MICROPOROUS MATERIALS WITH NEGATIVE POISSON RATIOS .2. MECHANISMS AND INTERPRETATION.* Journal of Physics D-Applied Physics, 1989. **22**(12): p. 1883-1887.

5. A.P. Pickles, K.L. Alderson, and K.E. Evans, *The effects of powder morphology on the processing of auxetic polypropylene (PP of negative Poisson's ratio).* Polymer Engineering and Science, 1996. **36**(5): p. 636-642.

6. K.L. Alderson and K.E. Evans, *THE FABRICATION OF MICROPOROUS POLYETHYLENE HAVING A NEGATIVE POISSON RATIO.* Polymer, 1992. **33**(20): p. 4435-4438.

7. M. Bianchi, F.L. Scarpa, and C.W. Smith, *Stiffness and energy dissipation in polyurethane auxetic foams.* Journal of Materials Science, 2008. **43**(17): p. 5851-5860.

8. K.L. Alderson, V.R. Simkins, V.L. Coenen, P.J. Davies, A. Alderson, and K.E. Evans, *How to make auxetic fibre reinforced composites.* Physica Status Solidi B-Basic Solid State Physics, 2005. **242**(3): p. 509-518.

9. H. Hu, Z. Wang, and S. Liu, *Development of auxetic fabrics using flat knitting*

technology. Textile Research Journal, 2011. **81**(14): p. 1493–1502.

10. C.T. Herakovich, *COMPOSITE LAMINATES WITH NEGATIVE THROUGH-THE-THICKNESS POISSON RATIOS.* Journal of Composite Materials, 1984. **18**(5): p. 447-455.
11. G.W. Milton, *COMPOSITE-MATERIALS WITH POISSON RATIOS CLOSE TO -1.* Journal of the Mechanics and Physics of Solids, 1992. **40**(5): p. 1105-1137.
12. L. Chen, C. Liu, J. Wang, W. Zhan, C. Hu, and S. Fan, *Auxetic materials with large negative Poisson's ratios based on highly oriented carbon nanotube structures.* APPLIED PHYSICS LETTERS, 2009. **94**.
13. P. Michelis and V. Spitas, *Numerical and experimental analysis of a triangular auxetic core made of CFR-PEEK using the Directionally Reinforced Integrated Single-yarn (DIRIS)Architecture* Composites Science and Technology, 2010. **70**: p. 1064–1071.
14. Z.Y. Ge and H. Hu, *A theoretical analysis of deformation behavior of an innovative 3D auxetic textile structure.* Journal of the Textile Institute, 2015. **106**(1): p. 101-109.
15. Z.Y. Ge, H. Hu, and Y.P. Liu, *Numerical analysis of deformation behavior of a 3D textile structure with negative Poisson's ratio under compression.* Textile Research Journal, 2015. **85**(5): p. 548-557.
16. Z.Y. Ge, H. Hu, and Y.P. Liu, *A finite element analysis of a 3D auxetic textile structure for composite reinforcement.* Smart Materials and Structures, 2013.

22(8): p. 8.

17. L.L. Jiang, B.H. Gu, and H. Hu, *Auxetic composite made with multilayer orthogonal structural reinforcement.* Composite Structures, 2016. **135**: p. 23-29.

18. L. Zhou, L.L. Jiang, and H. Hu, *Auxetic composites made of 3D textile structure and polyurethane foam.* Physica Status Solidi B-Basic Solid State Physics, 2016. **253**(7): p. 1331-1341.

19. K.E. Evans, M.A. Nkansah, and I.J. Hutchinson, *Modelling negative poisson ratio effects in network-embedded composites.* Acta Metallurgica et Materialia, 1992. **40**(9): p. 2463-2469.